

# Moisture infiltration characteristics of capillary barrier covers constructed with PAM-modified quarry waste

Litong Ji<sup>1</sup>, Lei Liu<sup>1,2,3</sup>, and Xingxing He<sup>2,3\*</sup>

<sup>1</sup>School of Mechanics and Engineering, Liaoning Technical University, Fuxin, Liaoning Province 123000, China

<sup>2</sup>State Key Laboratory of Geomechanics and Geotechnical Engineering Safety, Institute of Rock and Soil Mechanics, Chinese Academy of Sciences, Wuhan 430071, China

<sup>3</sup>Hubei Province Key Laboratory of Contaminated Sludge and Soil Science and Engineering, Wuhan 430071, China

**Abstract:** To improve the impermeability, water-retention capacity, and ecological suitability of quarry waste covers, an artificial ecological soil was prepared from typical waste rock collected from a quarry in Ezhou, Hubei Province, China. A capillary-barrier cover consisting of coarse and fine soil layers was then constructed, and the fine layer was amended with anionic polyacrylamide (PAM) to enhance its water-holding and seepage-control performance. Indoor soil-column infiltration experiments were conducted to examine the effects of PAM dosage, namely 0% (T1), 0.3% (T2), and 0.6% (T3), on volumetric water content and matric suction at different depths during rainfall infiltration. The results showed that PAM markedly delayed wetting-front migration and increased water storage within the cover layer. At a depth of 7.5 cm, wetting-front arrival times were 0.35 h, 0.59 h, and 1.67 h for T1, T2, and T3, respectively; at 30 cm, the corresponding values were 1.91 h, 3.06 h, and 6.21 h. Distinct water accumulation and backflow occurred at the capillary-barrier interface, where the peak volumetric water content increased from 39.93% in T1 to 46.04% in T2 and 48.53% in T3. Interface breakthrough time also increased with PAM dosage, reaching 4.28 h, 6.81 h, and 13.38 h, respectively. Overall, PAM-modified capillary-barrier covers effectively reduced infiltration and enhanced interfacial water retention, providing a basis for anti-seepage design and ecological restoration of quarry waste cover systems.

## 1 Introduction

With the expansion of the global construction industry, mining operations generate vast quantities of waste rock. In China, the building materials and mining sectors produce hundreds of millions of tons of solid waste annually, primarily stored in quarry waste [1]. Constrained by management conditions, land occupation and environmental pollution issues are prominent. The loose structure and exposed surface of waste piles make them susceptible to soil erosion and particle migration under rainfall and wind, intensifying risks of sediment-laden runoff and seepage. Simultaneously, potential heavy metals and harmful ions in waste residues may leach into water bodies with precipitation, threatening soil quality and ecological safety. Long-term improper stockpiling also alters soil physicochemical properties, hinders vegetation recovery and biodiversity, and undermines ecosystem stability[2-4].

For ecological restoration of waste rock dumps, soil reconstruction and vegetation recovery are critical components. The soil and water conservation effects of vegetation are primarily manifested in the following ways: the canopy intercepts rainfall and reduces the kinetic energy

of raindrops, thereby lowering runoff generation rates and erosion intensity; surface cover (vegetation and litter) increases roughness and slows runoff; root systems stabilize soil and improve soil structure, enhancing aggregate stability and pore connectivity, increasing water retention capacity, and consequently reducing the risk of soil erosion[5, 6].

Soil amendments enhance soil porosity, hydrological properties, pH, and nutrient environments while regulating microbial activity. They promote vegetation restoration and aggregate stability, thereby reducing soil erosion. Classified by origin, they include natural, synthetic, and composite types. To address issues like loose, erosion-prone cover soils in mine waste dumps, soil amendments are commonly used for stabilization. Among these, PAM demonstrates significant potential for structural improvement and erosion control in waste rock cover layers. Its excellent flocculation and binding properties promote fine particle aggregation, enhance structural stability, and regulate infiltration-runoff processes. This action reduces runoff scouring and sediment production, making PAM a promising solution for these challenges[7-9].

Capillary-blocking ecological barriers typically consist of an upper layer of fine-grained soil overlying a

\*Corresponding author: Xingxing He (xxhe@whrsm.ac.cn)

lower layer of coarse-grained soil. By exploiting the significant differences in hydraulic conductivity properties—such as permeability coefficient and hydraulic conductivity between the two layers under unsaturated conditions, infiltrating water becomes blocked at the interface. This causes water to be preferentially retained within the fine-grained layer, thereby achieving water storage and seepage prevention functions[10, 11]. Compared to traditional compacted clay and geomembrane-GCL composite cover systems, this system features a relatively simple structure, lower cost, easier maintenance, and stable impermeability performance. Consequently, it has been widely adopted for final cover applications in landfills across arid and semi-arid regions[12]. Early studies elucidated the control of water flow paths by sudden changes in hydraulic conductivity within unsaturated slopes and revealed the phenomenon of capillary blockage. Subsequent material combination and structural optimization tests demonstrated that composite coarse-fine-grained materials are more effective than single-fine-grained materials in forming an efficient capillary barrier. Furthermore, the gradation and uniformity of the underlying coarse-grained layer significantly influence the blockage efficiency[13, 14]. With theoretical advancements, research focus has gradually shifted toward long-term service performance evaluation, primarily conducted through field monitoring, laboratory permeability tests, and numerical simulations. Field test results from multiple locations indicate that capillary-blocking liners exhibit good impermeability in arid, semi-arid, and some semi-humid climates, typically with low seepage rates. However, in humid climates, sustained high infiltration and near-saturated conditions weaken the interfacial blocking effect, potentially increasing bottom seepage and reducing the liner's impermeability advantage compared to arid regions[15-17]. Overall, capillary-blocking cover layers achieve impermeability levels comparable to traditional covers in suitable climates while offering engineering economy and maintainability advantages. However, further research is needed to define their applicability boundaries and optimize structural parameters in humid regions.

Therefore, this study utilized quarry waste from building material mines as the primary material for artificial soil. Through indoor soil column tests, a three-layer functional structure of capillary-retention type cover was constructed, and its impermeability and resistance to rain erosion were systematically evaluated. Key parameter analysis and performance verification demonstrated that this cover system not only meets current standards for mine closure systems but also achieves effective water retention and ecological restoration. The findings provide technical support for resource utilization of industrial quarry waste and for implementing impermeability, water retention, and ecological restoration within cover systems.

## 2 Materials and Methods

### 2.1 Experimental Materials

Primary materials were collected from a typical waste-rock

dump in Ezhou, Hubei Province, China. Based on preliminary tests, an artificial soil was prepared by mixing conglomerate, weathered basalt, and mudstone at a mass ratio of 1:0.6:0.4. After crushing and screening, the fraction smaller than 2 mm was used to as the fine-grained layer, while the 2-5mm fraction simulated the coarse-grained layer in the cover layer. PAM with a molecular weight of 12million was selected as the modifier. The process is shown in Fig 1.

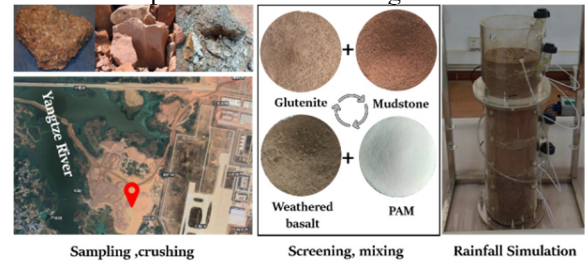


Fig. 1. Material preparation

### 2.2 Experiment apparatus

The experimental apparatus consisted of a soil-column rainfall simulation system, including a transparent acrylic column with an inner diameter of 180 mm and a height of 700 mm, a needle-type rainfall simulator, EC-5 soil moisture sensors for monitoring volumetric water content at different depths, tubular mini-tensiometers for measuring matric suction, a paperless data logger for continuous data acquisition, and an adjustable peristaltic pump for controlling rainfall intensity, as shown in Fig 1.

### 2.3 Experimental procedure

Artificial soil was prepared and amended with PAM at mass fractions of 0, 0.3%, and 0.6%, with all specimens initialized at a volumetric water content of 5%. The selected PAM dosages were determined with reference to previous studies showing that effective PAM contents for soil improvement generally fall within a low dosage range, commonly about 0.1%-1.0% by dry mass, while contents around 0.5% are often reported to provide pronounced improvements in water retention, cracking resistance, and barrier performance[18, 19]. Therefore, 0.3% and 0.6% were chosen as representative moderate and relatively high amendment levels to evaluate the dosage-dependent effects of PAM on infiltration and water-retention behavior. The bottom of the column was lined with permeable gauze, followed by a 20 cm thick coarse layer of 2-5 mm quarry waste, which was allowed to settle and then lightly compacted. A gauze separator was placed above the coarse layer, and the fine layer was packed in 5 cm lifts to a target dry density of 1.45 g cm<sup>-3</sup>, with each lift scarified before the next was added. PAM-modified soils were prepared in the same manner. After two layers of gauze were placed on the surface and a drainage outlet was installed for runoff collection, the column was sealed and stored indoors away from direct light until moisture equilibration was achieved. Rainfall infiltration tests were subsequently conducted using a pinhole rainfall simulator at an intensity of 20 mm h<sup>-1</sup>.

According to historical meteorological data from Ezhou, Hubei Province, this value is close to the short-duration rainstorm intensity for a 3-year return period and can therefore represent a typical extreme rainfall condition likely to be experienced by solid-waste dump covers during service. Thus, the selected rainfall intensity is of clear engineering relevance and experimental significance. Rainfall intensity was controlled using a peristaltic pump. The process is shown in Fig 2.

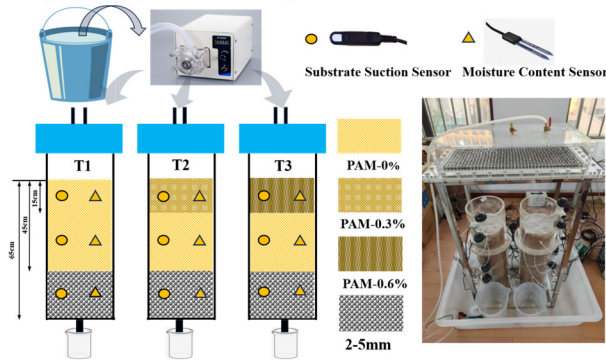


Fig. 2. Schematic of the rainfall infiltration test design

### 3 Analysis of experiment results

#### 3.1 Wetting front analysis

The wetting front is the distinct boundary between the advancing wetted zone and the underlying dry soil during infiltration, representing water migration driven by matric suction and gravity. Its advance rate indicates the soil's water-transport capacity and is a key metric for quantifying moisture movement within the structural layer under simulated rainfall[20, 21].

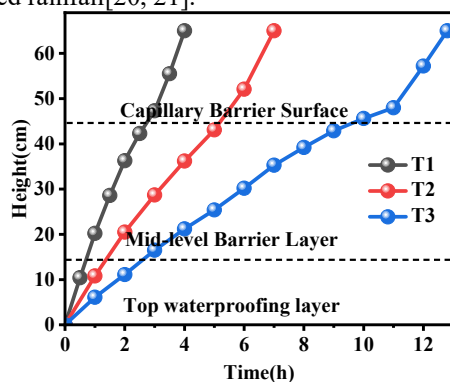


Fig. 3. Wetting-front migration curves of the PAM-modified quarry waste capillary-barrier structural layer

Fig 3 shows that increasing PAM content in the upper fine-grained layer delayed the arrival of the wetting front at the capillary-barrier interface. Relative to the control (T1), the interface arrival time increased by 2.32 h for T2 and 8.45 h for T3, corresponding to increases of 61.2% and 222.9%, respectively, and the overall wetting-front advance rate decreased. This response is attributed to PAM hydrogel formation, which occludes pore spaces, reduces effective porosity, and lowers hydraulic conductivity. After the wetting front reached the interface at 45 cm, the migration rate decreased initially and then increased. The coarse layer

has larger pores and lower capillary suction, which limits downward infiltration and causes water to accumulate at the interface. This promotes lateral redistribution and temporary storage within the fine layer, producing a pronounced capillary-barrier effect with localized backflow.

#### 3.2 Volume water content and runoff

As shown in Fig 5, volumetric water content exhibited clear depth-dependent and stage-wise responses to rainfall, and the evolution was strongly controlled by PAM dosage. All sensors recorded an initial water content of approximately 5 percent, consistent with the preset condition. The 7.5 cm sensor responded first, and wetting-front arrival was progressively delayed with increasing PAM, from 0.35 h in T1 to 0.59 h in T2 and 1.67 h in T3, indicating a marked reduction in infiltration rate. Consistent with the runoff in Fig 4. This retardation is attributed to PAM hydration and gel formation, which decreases effective pore space and hydraulic conductivity, promoting near-surface water accumulation and increased runoff.

After breakthrough of the upper fine layer, the 30 cm sensor responded, with arrival times of 1.91 h for T1, 3.06 h for T2, and 6.21 h for T3, indicating that PAM significantly retarded downward percolation. When the wetting front approached the fine-coarse interface, a distinct capillary-barrier effect emerged, as evidenced by rapid water accumulation and transient upward redistribution near the interface. Mechanistically, this phenomenon resulted from the hydraulic contrast between the two layers: the fine layer maintained relatively high matric suction, whereas the coarse layer, owing to its larger pore size, provided insufficient capillary force to draw water downward under unsaturated conditions. This mismatch in unsaturated hydraulic conductivity caused infiltration water to perch above the interface until the pressure conditions became sufficient for breakthrough. During this period, the accumulated water was partially redistributed upward in response to the matric potential gradient, giving rise to the observed backflow behavior. Peak water contents near the interface increased from 39.93% in T1 to 46.04% in T2 and 48.53% in T3, indicating that PAM enhanced interfacial water storage. This enhancement was likely associated with the improved water retention and reduced hydraulic conductivity of the PAM-modified fine layer, which further delayed breakthrough into the coarse layer.

Once interfacial water content exceeded the retention capacity of the capillary barrier, breakthrough occurred and the coarse layer began to wet, accompanied by a rapid decline in water content within the overlying fine layer due to gravitational drainage. The onset of seepage at the column outlet was delayed from 4.28 h in T1 to 6.81 h in T2 and 13.38 h in T3. Overall, PAM increased both the duration of non-saturated conditions and the maximum interfacial water storage, while substantially delaying wetting-front advance and seepage, with stronger effects at higher dosages.

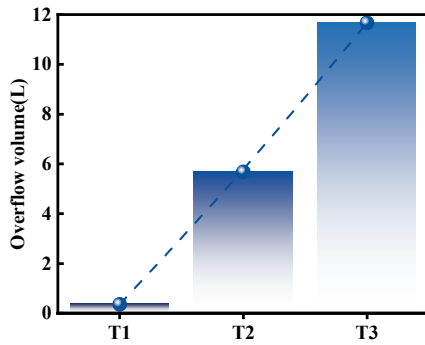


**Fig. 4.** Runoff volume from the PAM-modified quarry waste capillary-barrier structural layer

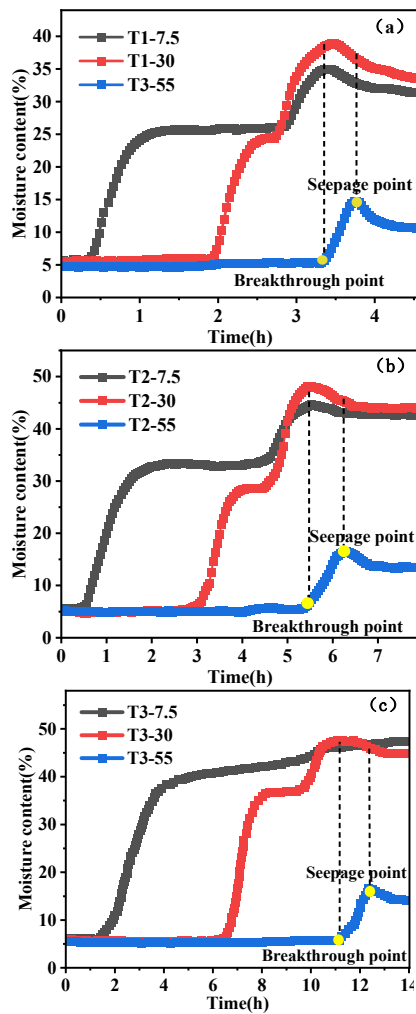


**Fig. 5.** Water infiltration curves of the PAM-modified quarry waste capillary-barrier structural layer: (a) 0% PAM; (b) 0.3% PAM; (c) 0.6% PAM

### 3.3 Matrix suction analysis

Since the matric suction sensors were installed at the same depths as the moisture sensors, temporal variations in matric potential effectively trace infiltration through the low-permeability layer. As shown in Fig 6, matric potential declined at all depths during rainfall and gradually approached 0 kPa, although the rate and amplitude differed with depth. This trend indicates progressive wetting and near-saturation of the structural layers by the end of

infiltration. The wetting-front advance was mirrored by a stepwise decline in matric suction, which corresponded to distinct infiltration stages.

The 7.5 cm sensor responded first, with suction rapidly decreasing toward 0 kPa. Initial suction decreased with increasing PAM dosage, measuring 86.92 kPa in T1, 76.65 kPa in T2, and 69.02 kPa in T3. This pattern is likely related to moisture redistribution during the equilibration period: the surface layer is susceptible to evaporative loss, which increases suction, whereas PAM improves water retention and limits desiccation, thereby maintaining lower initial suction.

A second pronounced suction drop occurred when the wetting front reached 25 cm, at 2.28 h for T1, 3.88 h for T2, and 8.01 h for T3, indicating that PAM increased hydraulic resistance and delayed downward wetting. As infiltration continued, suction in the middle fine layer further declined as water accumulated above the fine-coarse interface under the capillary-barrier effect, approaching 0 kPa as the layer neared saturation. After interface breakthrough, gravitational drainage caused a slight suction rebound. Finally, a sharp decrease in suction at 50 cm marked full structural breakthrough, occurring at 3.79 h, 6.11 h, and 12.24 h for T1, T2, and T3, respectively, consistent with breakthrough and seepage times inferred from the moisture records.

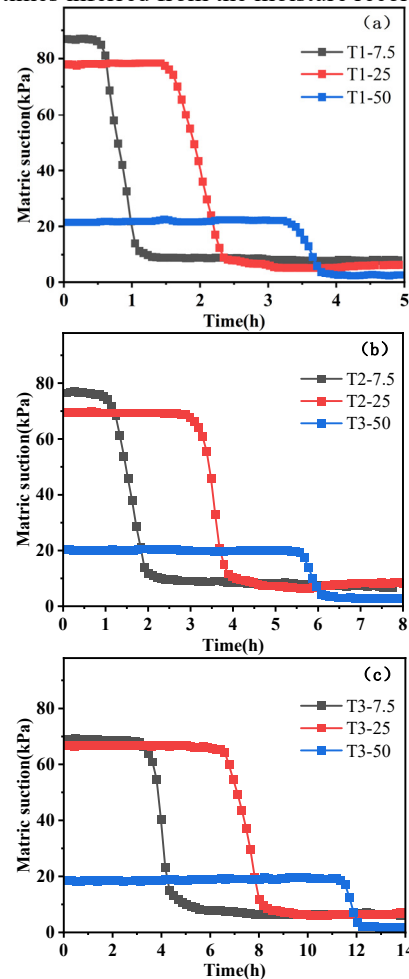


**Fig. 6.** Matric suction variation curves of the PAM- modified quarry waste capillary-barrier structural layer: (a) 0% PAM; (b) 0.3% PAM; (c) 0.6% PAM

### 3.4 Discussion

PAM has been widely used in agriculture and environmental management for erosion control, infiltration regulation, and water conservation, and has also shown potential in ecological restoration and slope rehabilitation. Previous studies have reported that PAM-based amendments can improve soil cohesion, enhance aggregate stability, and create more favorable moisture conditions for vegetation establishment, especially under relatively dry conditions. This is particularly important during seed germination and early seedling growth, when the cover substrate is most vulnerable to drying and instability[22]. In the present study, PAM improved water retention in the fine layer and promoted moisture accumulation near the fine-coarse interface, which could help support early plant establishment in quarry waste covers. Although the effect of PAM may gradually weaken under repeated wetting-drying cycles and long-term environmental exposure, its engineering value remains meaningful[23]. Once vegetation is established and the cover system becomes more stable through root development and soil evolution, the ecological function of the system may become less dependent on PAM itself.

However, the soil-column tests in this study only simulated a simplified one-dimensional infiltration process, whereas actual cover systems are influenced by a range of additional factors, including rainfall variability, evaporation, vegetation cover, and slope effects. Even so, the capillary-barrier concept has a solid engineering basis. This technique has been widely studied and applied in landfill and waste-cover systems, particularly in arid and semi-arid regions, where it has proven effective in reducing percolation and retaining moisture in the upper layer[24, 25]. Against this background, applying the same concept to quarry ecological restoration is both reasonable and practically meaningful. The main innovation of this study lies in combining the capillary-barrier structure with artificial soil derived from quarry waste and PAM modification, thereby providing an important basis for the development of cover systems that integrate seepage control with ecological restoration. Nevertheless, further studies are still required to evaluate long-term durability, field-scale hydraulic behavior, and ecological adaptability under natural environmental conditions, with the aim of improving the reliability and practical applicability of this technology in quarry restoration.

### 4 Conclusion

A capillary-barrier cover system was constructed using quarry waste-derived artificial soil, and the effects of PAM amendment on rainfall infiltration behavior were investigated through indoor soil-column experiments. The results showed that PAM significantly delayed wetting-front migration, reduced downward percolation, and increased water storage within the cover layer. A distinct capillary-barrier effect developed at the fine-coarse interface, where water accumulation and temporary upward redistribution were observed before breakthrough. With increasing PAM dosage, both the peak volumetric water

content and the breakthrough time at the interface increased, indicating enhanced interfacial water retention and seepage resistance. Overall, PAM-modified capillary-barrier covers can effectively improve the hydraulic performance of quarry waste cover systems and show promising potential for anti-seepage design and ecological restoration in quarry areas.

### Acknowledgments

The authors gratefully acknowledge the financial support from the National Key Research and Development Program of China (Grant No. 2024YFC3909303) and the National Natural Science Fund for Excellent Young Scientists (Grant No. 52322810).

### References

1. J. Zhang, K. Yang, X. He, X. Zhao, Z. Wei, S. He, *Research status of comprehensive utilization of coal-based solid waste (CSW) and key technologies of filling mining in China: A review*, Science of The Total Environment, **926** (2024) 171855.
2. H. Zhu, J. Xu, B. Zhou, J. Ren, Q. Yang, Z. Wang, W. Nie, *Leaching Characteristics of Potentially Toxic Metals from Tailings at Lujiang Alum Mine, China*, **19**(24) (2022) 17063.
3. W. Xiao, H. Ren, T. Sui, H. Zhang, Y. Zhao, Z. Hu, *A drone- and field-based investigation of the land degradation and soil erosion at an opencast coal mine dump after 5 years' evolution of natural processes*, International Journal of Coal Science & Technology, **9**(1) (2022) 42.
4. Y. Li, G. Lv, D. Wang, W. Su, Z. Wei, *Erosion Failure of Slope in a Dump with Ground Fissure under Heavy Rain*, **14**(21) (2022) 3425.
5. J. Liu, G. Gao, S. Wang, L. Jiao, X. Wu, B. Fu, *The effects of vegetation on runoff and soil loss: Multidimensional structure analysis and scale characteristics*, Journal of Geographical Sciences, **28**(1) (2018) 59-78.
6. S. Wei, K. Zhang, C. Liu, Y. Cen, J. Xia, *Effects of different vegetation components on soil erosion and response to rainfall intensity under simulated rainfall*, CATENA, **235** (2024) 107652.
7. A.A. Albalasmeh, E.H. Hamdan, M.A. Gharaibeh, A.E. Hanandeh, *Improving aggregate stability and hydraulic properties of Sandy loam soil by applying polyacrylamide polymer*, Soil and Tillage Research, **206** (2021) 104821.
8. B. Kebede, A. Tsunekawa, N. Haregeweyn, A.I. Mamedov, M. Tsubo, A.A. Fenta, D.T. Meshesha, T. Masunaga, E. Adgo, G. Abebe, M.L. Berihun, *Effectiveness of Polyacrylamide in Reducing Runoff and Soil Loss under Consecutive Rainfall Storms*, **12**(4) (2020) 1597.
9. C. Ao, P. Yang, W. Zeng, W. Chen, Y. Xu, H. Xu, Y. Zha, J. Wu, J. Huang, *Impact of raindrop diameter*

- and polyacrylamide application on runoff, soil and nitrogen loss via raindrop splashing*, *Geoderma*, **353** (2019) 372-381.
10. T. Miyazaki, *Water flow in unsaturated soil in layered slopes*, *Journal of Hydrology*, **102**(1) (1988) 201-214.
  11. W. Huo, Z. Zhu, J. Hao, W. Zhang, Y. Peng, *Experimental study and numerical simulation on effectiveness of different capillary barriers in silt low subgrade*, *Bulletin of Engineering Geology and the Environment*, **81**(6) (2022) 246.
  12. J X. Li, X. Li, F. Wang, Y. Liu, *The design criterion for capillary barrier cover in multi-climate regions*, *Waste Management*, **149** (2022) 33-41.
  13. C. Gao, Y. Zhu, Y. Zhang, *Stability Analysis of the Inclined Capillary Barrier Covers under Rainfall Condition*, **12**(8) (2022) 1218.
  14. A. Aslan Fidan, M.M. Berilgen, *Effect of the Mid-Layer on the Diversion Length and Drainage Performance of a Three-Layer Cover with Capillary Barrier*, **14**(1) (2024) 21.
  15. H. Guo, C.W.W. Ng, Q. Zhang, C. Qu, L. Hu, *Modelling the water diversion of a sustainable cover system under humid climates*, *Journal of Rock Mechanics and Geotechnical Engineering*, **16**(7) (2024) 2429-2440.
  16. A.M. Abdolazadeh, B. Lacroix Vachon, A.R. Cabral, *Assessment of the Design of an Experimental Cover with Capillary Barrier Effect Using 4 Years of Field Data*, *Geotechnical and Geological Engineering*, **29**(5) (2011) 783-802.
  17. C. Gao, W.-M. Ye, P.-H. Lu, Z.-R. Liu, Q. Wang, Y.-G. Chen, *An infiltration model for inclined covers with consideration of capillary barrier effect*, *Engineering Geology*, **326** (2023) 107318.
  18. Y.-Z. Bi, J.-M. Wen, H.-L. Wu, Y.-J. Du, *Evaluation of Performance of Polyacrylamide-Modified Compacted Clay as a Gas Barrier: Water Retention and Gas Permeability and Diffusion Characteristics*, **12**(16) (2022) 8379.
  19. T. Zhang, Y. Deng, H. Lan, F. Zhang, H. Zhang, C. Wang, Y. Tan, R. Yu, *Experimental Investigation of the Compactability and Cracking Behavior of Polyacrylamide-Treated Saline Soil in Gansu Province, China*, **11**(1) (2019) 90.
  20. Y. Sun, Y. Yang, B. Zhang, X. Zhang, Y. Xu, Y. Xiang, J. Chen, *Applicability of the Modified Green-Ampt Model Based on Suction Head Calculation in Water-Repellent Soil*, **15**(16) (2023) 2925.
  21. T. Thyagaraj, U. Salini, *Effect of pore fluid osmotic suction on matric and total suctions of compacted clay*, *Géotechnique*, **65**(11) (2015) 952-960.
  22. Z. Lu, C. Yu, H. Liu, J. Zhang, Y. Zhang, J. Wang, Y. Chen, *Application of New Polymer Soil Amendment in Ecological Restoration of High-Steep Rocky Slope in Seasonally Frozen Soil Areas*, **16**(13) (2024) 1821.
  23. Y.-C. Cheng, C.-P. Wang, K.-Y. Liu, S.-Y. Pan, *Towards sustainable management of polyacrylamide in soil-water environment: Occurrence, degradation, and risk*, *Science of The Total Environment*, **926** (2024) 171587.
  24. C.W.W. Ng, H. Guo, J. Ni, R. Chen, Q. Xue, Y. Zhang, Y. Feng, Z. Chen, S. Feng, Q. Zhang, *Long-term field performance of non-vegetated and vegetated three-layer landfill cover systems using construction waste without geomembrane*, *Géotechnique*, **74**(2) (2022) 155-173.
  25. C.W.W. Ng, H. Guo, J. Ni, Q. Zhang, R. Chen, Y. Zhang, *Effects of plant-biochar interaction on the performance of a landfill cover system: field monitoring and numerical modelling*, **60**(11) (2023) 1663-1680.